Acta Crystallographica Section F
Structural Biology and Crystallization Communications
ISSN 1744-3091

Crystallization and preliminary X-ray analysis of human MTH1 complexed with two oxidized nucleotides, 8-oxo-dGMP and 2-oxo-dATP

Teruya Nakamura,[a] Yuki Kitaguchi,[a] Masayuki Miyazawa,[a] Hiroyuki Kamiya,[b] Sachiko Toma,[a] Shinji Ikemizu,[a] Masahiro Shirakawa,[c] Yusaku Nakabeppu[d] and Yuriko Yamagata[a]*

[a]Graduate School of Pharmaceutical Sciences, Kumamoto University, Kumamoto 862-0973, Japan, [b]Graduate School of Pharmaceutical Sciences, Hokkaido University, Sapporo 060-0812, Japan, [c]Graduate School of Engineering, Kyoto University, Kyoto 615-8510, Japan, and [d]Medical Institute of Bioregulation, Kyushu University, Fukuoka 812-8582, Japan

Correspondence e-mail: yamagata@gpo.kumamoto-u.ac.jp

Received 16 October 2006
Accepted 19 November 2006

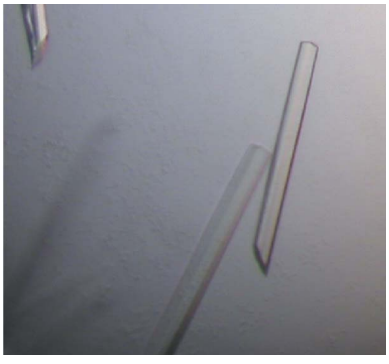

Human MutT homologue 1 (hMTH1) hydrolyzes a variety of oxidized purine nucleoside triphosphates, including 8-oxo-dGTP, 2-oxo-dATP, 2-oxo-ATP and 8-oxo-dATP, to their corresponding nucleoside monophosphates, while *Escherichia coli* MutT possesses prominent substrate specificity for 8-oxoguanine nucleotides. Three types of crystals were obtained corresponding to the following complexes: selenomethionine-labelled hMTH1 with 8-oxo-dGMP (SeMet hMTH1–8-oxo-dGMP), hMTH1 with 8-oxo-dGMP (hMTH1–8-oxo-dGMP) and hMTH1 with 2-oxo-dATP (hMTH1–2-oxo-dATP). Crystals of the SeMet hMTH1–8-oxo-dGMP complex belong to space group $P4_12_12$, with unit-cell parameters $a = b = 45.8$, $c = 153.6$ Å, and diffracted to 2.90 Å. Crystals of hMTH1–8-oxo-dGMP and hMTH1–2-oxo-dATP belong to space groups $P2_1$ and $P2_12_12_1$, with unit-cell parameters $a = 34.0$, $b = 59.0$, $c = 65.9$ Å, $\beta = 90.7^\circ$ and $a = 59.2$, $b = 67.3$, $c = 80.0$ Å, respectively. Their diffraction data were collected at resolutions of 1.95 and 2.22 Å, respectively.

1. Introduction

Reactive oxygen species that are produced during normal cellular metabolism damage DNA, RNA and their precursor nucleotides and generate various modified bases. Of these bases, 8-oxoguanine (8-oxoG), which is generated by attack of oxygen at the C8 position of guanine, possesses a high mutagenic potency owing to its mispairing with adenine. The *Escherichia coli* MutT protein (129 amino acids, M_r = 14 927; GenBank X04831) hydrolyzes 8-oxo-dGTP and 8-oxo-GTP to their corresponding monophosphates and prevents A:T to C:G transversion mutations and abnormal protein synthesis caused by the misincorporation of 8-oxoG into DNA or RNA (Maki & Sekiguchi, 1992; Taddei *et al.*, 1997). The mammalian counterpart of MutT, MutT homologue 1 (MTH1), has been identified in human cells (Sakumi *et al.*, 1993). MutT and MTH1 belong to the Nudix (nucleoside diphosphate linked to some other moiety *X*) hydrolase superfamily that contains the conserved MutT signature (Nudix motif) GX_5EX_7RE*UX*EE*X*G*U* (where *U* is a hydrophobic residue; Bessman *et al.*, 1996). Only 26 amino-acid residues are identical (20% sequence identity) between *E. coli* MutT and human MTH1 (hMTH1; 156 amino acids; M_r = 17 951; GenBank D38594) in spite of the highly conserved MutT signature in which 13 of 23 amino-acid residues are identical.

Both MutT and MTH1 prevent A:T to C:G transversion mutations by removing mutagenic oxidized nucleotides. However, there are several differences in substrate specificity between the two homologues. MutT has a 14 000-fold higher affinity for 8-oxo-dGTP than for dGTP (Ito *et al.*, 2005). On the other hand, hMTH1 has a lower substrate specificity for 8-oxo-dGTP than MutT. The K_m value of hMTH1 for 8-oxo-dGTP is only approximately 20-fold lower than that for dGTP (Fujikawa *et al.*, 1999). In addition, hMTH1 hydrolyzes the oxidized adenine nucleotides 2-oxo-dATP, 2-oxo-ATP and 8-oxo-dATP. The k_{cat}/K_m values for 8-oxo-dGTP, 2-oxo-dATP, 2-oxo-ATP and 8-oxo-dATP are 0.81, 1.68, 1.09 and 0.78 s^{-1} μM^{-1}, respectively (Fujikawa *et al.*, 1999, 2001). Previous reports have shown that 2-oxoadenine (2-oxoA, also known as isoguanine) can induce G:C to T:A transversion mutations (Inoue *et al.*, 1998) and that 2-oxoA was

not generated in DNA by the direct oxidation of adenine but by the misincorporation of 2-oxo-dATP into the DNA (Kamiya & Kasai, 1995). Therefore, similar to the 8-oxo-dGTPase activity, the strong 2-oxo-dATPase activity of hMTH1 also contributes to the prevention of transversion mutations (Yoshimura *et al.*, 2003). Mice that lack the *mth1* gene exhibit an increased occurrence of spontaneous carcinogenesis, especially in the liver and, to a lesser extent, in the lungs and stomach; this suggests that the accumulation of oxidized purine nucleotides triggers such malignant transformation *in vivo* (Tsuzuki *et al.*, 2001).

Mutational analyses and NMR structures of hMTH1 suggest that Phe27, Trp117, Asp119 and Asn33 are the active-site residues associated with the recognition of 8-oxo-dGTP and 2-oxo-dATP; however, their mutants have different effects on the catalysis of 8-oxo-dGTP and 2-oxo-dATP (Sakai *et al.*, 2002; Yoshimura *et al.*, 2003; Mishima *et al.*, 2004). For example, Asp119 is probably a key residue for the selective recognition of 2-oxo-dATP, because the D119A mutant completely abolishes the 2-oxo-dATPase activity but retains approximately 50% of the activity of the wild type with respect to 8-oxo-dGTPase (Yoshimura *et al.*, 2003). However, we could not propose a mechanism of substrate recognition by hMTH1 on the basis of these mutational and NMR data and crystallographic studies have not yet been reported. Thus, the crystal structures of hMTH1 complexed with its substrates and products are essential in order to obtain structural insights into the broad substrate specificity of hMTH1, which differs significantly from that of *E. coli* MutT.

This is the first report on the crystallization and preliminary X-ray crystallographic analysis of hMTH1 complexed with the oxidized nucleotides 8-oxo-dGMP and 2-oxo-dATP.

2. Protein expression and purification

The full-length hMTH1 protein with no tags was expressed and purified as described previously (Mishima *et al.*, 2004) with minor modifications. Native hMTH1 was overexpressed by transforming the pET8c/hMTH1 plasmid into *E. coli* strain BL21(DE3) cells cultured in LB broth. SeMet-labelled hMTH1 was overexpressed under conditions of methionine-pathway inhibition (Doublié, 1997) in LeMaster Broth (LeMaster & Richards, 1985). Gel-filtration chromatography was performed using a HiLoad 16/60 Superdex 75 pg column (Amersham Biosciences) instead of a Sephacryl S-100 column (Mishima *et al.*, 2004). The purified native protein and the SeMet derivative were concentrated to 6–12 mg ml^{-1} in 20 m*M* Tris–HCl pH 7.5 and 5% glycerol and to 2–4 mg ml^{-1} in 20 m*M* Tris–HCl pH 7.5, respectively. 8-oxo-dGMP and 2-oxo-dATP were prepared as described previously (Nakamura *et al.*, 2004; Kamiya & Kasai, 1995) and dissolved in water.

3. Crystallization

The complexes were crystallized using the sitting-drop vapour-diffusion method for SeMet-labelled hMTH1 with 8-oxo-dGMP (SeMet hMTH1–8-oxo-dGMP) and using the hanging-drop vapour-diffusion method for hMTH1 with 8-oxo-dGMP (hMTH1–8-oxo-dGMP) and hMTH1 with 2-oxo-dATP (hMTH1–2-oxo-dATP). The crystallization conditions for hMTH1–8-oxo-dGMP were initially screened at 288 K using the Hampton Crystal Screen 2, Lite and Grid Screen PEG 6000 kits. 1 µl of a solution containing the protein and 8-oxo-dGMP was mixed with an equal volume of reservoir solution and the mixture was equilibrated against 0.3 ml reservoir solution. Clustered thin needle-shaped crystals were produced in a droplet made from a solution containing 0.1 *M* citric acid pH 4.0 and 20%(*w*/*v*) polyethylene glycol (PEG) 6000 that was provided in the Grid Screen PEG 6000 kit. Subsequently, single crystals of SeMet hMTH1–8-oxo-dGMP were grown over 10 d in a droplet that contained 2 µl each of protein solution (2 mg ml^{-1}) containing 1.5 m*M* 8-oxo-dGMP and reservoir solution [100 m*M* citric acid pH 4.0 and 18%(*w*/*v*) PEG 6000] equilibrated against 0.3 ml reservoir solution (Fig. 1*a*). Single crystals of hMTH1–8-oxo-dGMP and hMTH1–2-oxo-dATP were obtained by streak-seeding and by altering the protein and PEG 6000 concentrations. Thin rod-shaped crystals of hMTH1–8-oxo-dGMP were grown over 1–3 d in a droplet that contained 0.6 µl 10 mg ml^{-1} protein, 0.9 µl 2.5 m*M* 8-oxo-dGMP and 1.5 µl reservoir solution [100 m*M* citric acid pH 4.0 and 20%(*w*/*v*) PEG 6000] equilibrated against 0.3 ml reservoir solution (Fig. 1*b*). Rod-shaped crystals of hMTH1–2-oxo-dATP grew over 1–3 d in a droplet that contained 0.5 µl 7 mg ml^{-1} protein, 1 µl 5 m*M* 2-oxo-dATP and 1.5 µl reservoir solution [100 m*M* citric acid pH 4.0 and 10%(*w*/*v*) PEG 6000] equilibrated against 0.3 ml reservoir solution (Fig. 1*c*).

4. Data collection and processing

All crystals were transferred into a cryoprotectant containing 0.1 *M* citric acid pH 4.0 and 30%(*w*/*v*) PEG 6000, mounted in a cryoloop (Hampton Research) and flash-frozen in a nitrogen stream at 100 K. Diffraction data sets for the three types of crystals were collected at beamlines BL38B1, BL40B2, BL41XU and BL44XU at SPring-8 (Harima, Japan) and beamline 6A at Photon Factory (Tsukuba, Japan). SeMet hMTH1–8-oxo-dGMP diffraction data were collected at four wavelengths (0.9799, 0.9801, 0.9959 and 0.9646 Å) for MAD

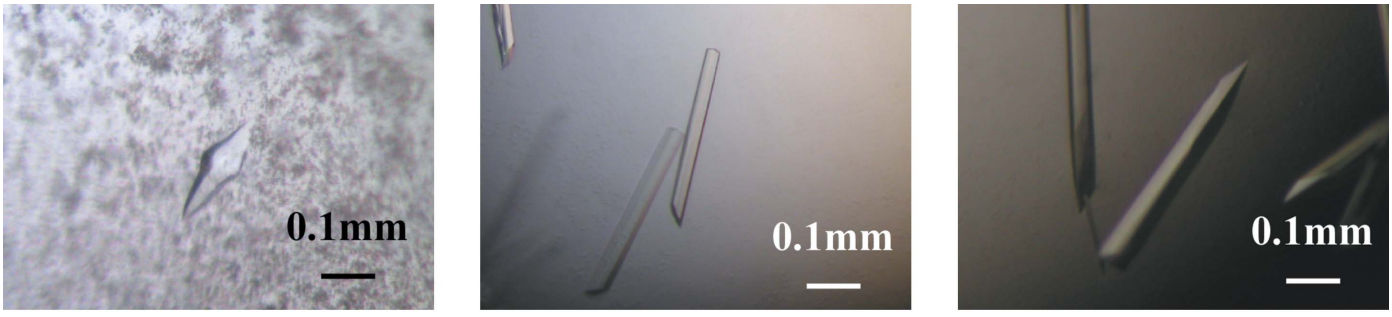

(*a*) (*b*) (*c*)

Figure 1
Crystals of hMTH1 complexed with oxidized nucleotides. (*a*) SeMet hMTH1–8-oxo-dGMP crystal with dimensions of 0.04 × 0.04 × 0.2 mm. (*b*) hMTH1–8-oxo-dGMP crystal with dimensions of 0.02 × 0.02 × 0.3 mm. (*c*) hMTH1–2-oxo-dATP crystal with dimensions of 0.04 × 0.05 × 0.4 mm.

Table 1
Data-collection statistics.

Values in parentheses correspond to the highest resolution shell.

Diffraction data	SeMet hMTH1–8-oxo-dGMP	hMTH1–8-oxo-dGMP	hMTH1–2-oxo-dATP
Beamline	SPring-8 BL38B1	SPring-8 BL44XU	PF BL6A
Wavelength (Å)	0.9959	0.9000	0.978
Space group	$P4_12_12$	$P2_1$	$P2_12_12_1$
Unit-cell parameters (Å, °)	$a = b = 45.8$, $c = 153.6$	$a = 34.0$, $b = 59.0$, $c = 65.9$, $\beta = 90.7$	$a = 59.2$, $b = 67.3$, $c = 80.0$
Resolution range (Å)	50.0–2.9 (3.00–2.90)	50.0–1.95 (2.02–1.95)	50.0–2.22 (2.30–2.22)
No. of observed reflections	52863	64087	116446
No. of unique reflections	6923	18663	16347
Completeness (%)	100 (100)	97.8 (88.2)	99.5 (98.8)
R_{merge}† (%)	7.9 (37.8)	6.3 (29.6)	4.8 (19.7)
$\langle I/\sigma(I)\rangle$	43.7 (7.8)	24.3 (3.0)	52.0 (12.2)

† $R_{merge} = 100 \times \sum |I_{hkl} - \langle I_{hkl}\rangle| / \sum I_{hkl}$, where $\langle I_{hkl}\rangle$ is the mean value of I_{hkl}.

phasing. All data were processed, integrated and scaled using *HKL*-2000 (Otwinowski & Minor, 1997). The SeMet hMTH1–8-oxo-dGMP crystals belong to space group $P4_12_12$ or $P4_32_12$, with unit-cell parameters $a = b = 45.8$, $c = 153.6$ Å ($\lambda = 0.9959$ Å). Assuming the presence of one complex per asymmetric unit, the Matthews coefficient V_M is 2.2 Å^3 Da^{-1} and the solvent content is estimated to be 45% (Matthews, 1968). In contrast, the native crystals of the hMTH1–8-oxo-dGMP complex belong to space group $P2_1$, with unit-cell parameters $a = 34.0$, $b = 59.0$, $c = 65.9$ Å, $\beta = 90.7°$, while those of the hMTH1–2-oxo-dATP complex belong to space group $P2_12_12_1$, with unit-cell parameters $a = 59.2$, $b = 67.3$, $c = 80.0$ Å. Assuming the presence of two molecules per asymmetric unit, the V_M values are 1.8 and 2.2 Å^3 Da^{-1} and the calculated solvent contents are 33 and 44% for hMTH1–8-oxo-dGMP and hMTH1–2-oxo-dATP, respectively. The data-collection statistics of the best data sets used for structure determination of the three types of crystals are provided in Table 1.

5. Crystallographic analysis

We initially attempted to solve the structure of SeMet hMTH1–8-oxo-dGMP by the MAD method, but the trial was unsuccessful. We then performed molecular replacement (MR) with the SeMet hMTH1–8-oxo-dGMP data ($\lambda = 0.9959$ Å) using the NMR structure of hMTH1 (PDB code 1iry) as a search model. Calculations were performed using *MOLREP* (Vagin & Teplyakov, 1997) with many modified models including removed loops and/or Ala-substituted residues. Significant solutions (correlation coefficient = 40–43% and *R* factor = 61–64%) were obtained for some models after translation-function calculations in space group $P4_12_12$ and $2F_o - F_c$ electron-density maps were calculated after positional refinement with *CNS* (Brünger *et al.*, 1998). Among these refined structures, a structure that contained 75% atoms ($R = 38.4\%$ and $R_{free} = 42.4\%$) yielded a better $2F_o - F_c$ map and almost the entire molecule could be traced using this map. Furthermore, the map also showed apparent density for a nucleotide in the substrate-binding pocket. The structures of hMTH1–8-oxo-dGMP and hMTH1–2-oxo-dATP were determined using the MR method with the *MOLREP* program (Vagin & Teplyakov, 1997). The partially refined SeMet hMTH1–8-oxo-dGMP structure was used as a search model. The $2F_o - F_c$ maps that were obtained from the models after *CNS* refinements revealed unambiguous density for 8-oxo-dGMP and 2-oxo-dATP in their respective substrate-binding sites.

This work was supported in part by Research Fellowships of the Japan Society for the Promotion of Science for Young Scientists (to TN), by Grants-in-Aid for Scientific Research on Priority Areas and by the National Project for Protein Structural and Functional Analysis from the Ministry of Education, Culture, Sports, Sciences and Technology of Japan.

References

Bessman, M. J., Frick, D. N. & O'Handley, S. F. (1996). *J. Biol. Chem.* **271**, 25059–25062.
Brünger, A. T., Adams, P. D., Clore, G. M., DeLano, W. L., Gros, P., Grosse-Kunstleve, R. W., Jiang, J.-S., Kuszewski, J., Nilges, M., Pannu, N. S., Read, R. J., Rice, L. M., Simonson, T. & Warren, G. L. (1998). *Acta Cryst.* D**54**, 905–921.
Doublié, S. (1997). *Methods Enzymol.* **276**, 523–530.
Fujikawa, K., Kamiya, H., Yakushiji, H., Fujii, Y., Nakabeppu, Y. & Kasai, H. (1999). *J. Biol. Chem.* **274**, 18201–18205.
Fujikawa, K., Kamiya, H., Yakushiji, H., Nakabeppu, Y. & Kasai, H. (2001). *Nucleic Acids Res.* **29**, 449–454.
Inoue, M., Kamiya, H., Fujikawa, K., Ootsuyama, Y., Murata-Kamiya, N., Osaki, T., Yasumoto, K. & Kasai, H. (1998). *J. Biol. Chem.* **273**, 11069–11074.
Ito, R., Hayakawa, H., Sekiguchi, M. & Ishibashi, T. (2005). *Biochemistry*, **44**, 6670–6674.
Kamiya, H. & Kasai, H. (1995). *J. Biol. Chem.* **270**, 19446–19450.
LeMaster, D. M. & Richards, F. M. (1985). *Biochemistry*, **24**, 7263–7268.
Maki, H. & Sekiguchi, M. (1992). *Nature (London)*, **355**, 273–275.
Matthews, B. W. (1968). *J. Mol. Biol.* **33**, 491–497.
Mishima, M., Sakai, Y., Itoh, N., Kamiya, H., Furuichi, M., Takahashi, M., Yamagata, Y., Iwai, S., Nakabeppu, Y. & Shirakawa, M. (2004). *J. Biol. Chem.* **279**, 33806–33815.
Nakamura, T., Doi, T., Sekiguchi, M. & Yamagata, Y. (2004). *Acta Cryst.* D**60**, 1641–1643.
Otwinowski, Z. & Minor, W. (1997). *Methods Enzymol.* **276**, 307–326.
Sakai, Y., Furuichi, M., Takahashi, M., Mishima, M., Iwai, S., Shirakawa, M. & Nakabeppu, Y. (2002). *J. Biol. Chem.* **277**, 8579–8587.
Sakumi, K., Furuichi, M., Tsuzuki, T., Kakuma, T., Kawabata, S., Maki, H. & Sekiguchi, M. (1993). *J. Biol. Chem.* **268**, 23524–23530.
Taddei, F., Hayakawa, H., Bouton, M., Cirinesi, A., Matic, I., Sekiguchi, M. & Radman, M. (1997). *Science*, **278**, 128–130.
Tsuzuki, T., Egashira, A., Igarashi, H., Iwakuma, T., Nakatsuru, Y., Tominaga, Y., Kawate, H., Nakao, K., Nakamura, K., Ide, F., Kura, S., Nakabeppu, Y., Katsuki, M., Ishikawa, T. & Sekiguchi, M. (2001). *Proc. Natl Acad. Sci. USA*, **98**, 11456–11461.
Vagin, A. & Teplyakov, A. (1997). *J. Appl. Cryst.* **30**, 1022–1025.
Yoshimura, D., Sakumi, K., Ohno, M., Sakai, Y., Furuichi, M., Iwai, S. & Nakabeppu, Y. (2003). *J. Biol. Chem.* **278**, 37965–37973.